

Enthalpic and Entropic Effects of Salt and Polyol Osmolytes on Site-Specific Protein–DNA Association: The Integrase Tn916–DNA Complex[†]

Stoyan Milev, Hans Rudolf Bosshard, and Ilian Jelesarov*

Biochemisches Institut der Universität Zürich, Winterthurerstrasse 190, CH-8057 Zürich, Switzerland

Received May 28, 2004; Revised Manuscript Received October 18, 2004

ABSTRACT: The effect of low molecular-weight compounds on the equilibrium constant K_A can be used to explore the energetics and molecular mechanism of protein–DNA interactions. Here we use the complex composed of the integrase Tn916 DNA-binding domain and its target DNA duplex to investigate the effects of salt and the nonionic osmolytes glycerol and sorbitol on sequence-specific protein–DNA association. Increasing Na^+ concentration from 0.12 to 0.32 M weakens the binding affinity by a factor of 20. The decrease of affinity is dominated by a large loss of binding enthalpy but only a small loss of binding entropy. This contrasts the concept that the salt-induced weakening of protein–DNA binding is mainly entropic. The large enthalpy loss is discussed in the light of recent views about the nature of the general salt effect. Addition of up to 2.5 M sorbitol and up to 3.3 M glycerol causes a slight increase of the binding affinity. However, both osmolytes lead to a large enthalpy gain and a similarly large entropy loss. This intriguing enthalpy–entropy compensation can be explained in part by an enthalpic chelate effect: The osmolyte tightens the structure of the protein–DNA complex whereby the formation of enthalpically favorable noncovalent interactions is promoted at the entropic cost of a more rigid complex. The results were obtained by isothermal titration calorimetry. They are supported by kinetic experiments showing that the rate of formation of the complex is reduced by salt, but the rate of complex dissociation is not. Glycerol and sorbitol reduce both rates in line with an only small effect on complex stability. This work clarifies the thermodynamic and kinetic response of a novel protein–DNA complex to increased salt and the presence of two common, nonionic osmolytes.

Protein–DNA complexes are held together by weak noncovalent forces: van der Waals contacts, hydrogen bonds, salt bridges, and long-range electrostatic interactions. These forces depend on temperature, pH, pressure, osmotic pressure, salt concentration, and other environmental variables. However, the straightforward application of concepts developed in the tradition of classical physical chemistry often fails to explain the strength of macromolecular association and its modulation by environmental parameters. This difficulty is underlined by many unsuccessful attempts to design potent ligands for biological macromolecules. One reason is that macromolecules interact with each other over vast molecular surface areas representing complementary arrays of highly cooperative bonding networks leading to significant hydration effects. Moreover, macromolecules are soft and flexible, and hence adaptable. Characterization of the effect of salts and osmolytes on the energetics and kinetics of macromolecular recognition is one way to deepen our understanding of the complex mechanisms by which associating macromolecules buffer environmental changes.

The effect of salt on the binding free energy (ΔG)¹ of protein–DNA interaction is long known and has been treated theoretically (1–4). The general, that is, the nonspecific, salt effect arises from the reorganization of the ionic cloud around

the DNA and the protein. Usually the binding affinity decreases when the salt concentration increases. However, experimental studies on the energetic partitioning of the salt effect in terms of enthalpy (ΔH) and entropy (ΔS) and on the influence of salt on the rate of binding and dissociation are controversial (5–18). It has been argued that the salt-induced loss of affinity is entropic, while the enthalpic effect is negligible (3, 9). In contrast, computational modeling of the solvation free energy of polyelectrolytes based on the nonlinear Poisson–Boltzmann equation indicates a considerable electrostatic enthalpy term contributing to the salt dependence of DNA–ligand binding (4). Indeed, direct calorimetric measurements have detected salt-induced losses of enthalpy in some protein–DNA complexes (6, 12, 15).

Water plays an important role in protein–DNA association (19). Structural and computational analyses have identified water molecules bridging protein and DNA and participating in hydrogen bonding networks (20–25). On the other hand, the intimate fit between protein and DNA surfaces is also accompanied by the release of water molecules. The osmotic stress technique is one way to quantify changes in hydration (26, 27). With some caveats, the free energy changes induced

[†] This work was supported in part by Grant 3100A0-100197/1 from the Swiss National Science Foundation.

* To whom correspondence should be addressed. Telephone: +41 1 655 5547. Fax: +41 1 635 6805. E-mail: iljel@bioc.unizh.ch.

¹ Abbreviations: bp, base pair; ΔG , free energy change; ΔH , enthalpy change; Int-DBD, DNA-binding domain of the Tn916 transposon integrase; ITC, isothermal titration calorimetry; K_A^{ITC} , equilibrium association constant from ITC; K_A^{kin} , equilibrium association constant from kinetic data; k_{on} , association rate constant; k_{off} , dissociation rate constant; ΔS , entropy change.

by osmolytes can be related to the number of osmotically labile water molecules (28, 29). However, one has to consider that osmolytes may stabilize or destabilize protein and DNA per se or preferentially interact with the free or bound state and thereby exert an indirect effect on the energetics of the protein–DNA complex. Altogether, osmolytes perturb in a complex way the energetics of the associating system.

Recently, we began to investigate the energetics of the reaction of the DNA binding domain of integrase Tn916 with its target DNA contained in a 13 bp DNA duplex. Tn916 is a promiscuous transposon element spreading resistance to tetracycline among pathogenic bacteria (30). Its excision and reintegration is carried out by the Tn916 integrase the N-terminal domain of which is responsible for DNA binding. We have chosen the integrase–DNA system since the structure of both the free DNA binding domain (Int-DBD) of Tn916 and the Int-DBD–DNA complex are known (31, 32). This information is a prerequisite for linking thermodynamic parameters with structure. Moreover, Int-DBD recognizes its target site by the face of a three-stranded β -sheet fitting into the major groove of the DNA (31, 32). This is a novel and rare DNA-binding motif. Information on structurally novel protein–DNA complexes is essential to achieve a deeper insight into the strategies used by proteins for DNA recognition. Therefore, comparison of the properties of the Int–DNA complex with those of other more common DNA-binding motifs is instructive. In our recent detailed thermodynamic characterization of the Int-DBD–DNA complex (33) and its components (34), we presented evidence for significant structural rearrangements accompanying complex formation. Adaptation occurs at the cost of introducing conformational disorder in parts of the integrase binding domain. Dehydration of the binding interface of Int-DBD is incomplete with several water molecules remaining bound at the protein–DNA contact site.

In the present study, we investigate the influence of salt and the nonionic, polyol osmolytes glycerol and sorbitol on the stability and the kinetics of formation of the Int-DBD–DNA complex. In particular, we separate the entropic and enthalpic effect of salt on the stability of the complex to clarify the thermodynamic origin of the salt effect. The main observation is that the salt-induced decrease of affinity is mainly of enthalpic nature, for which we put forward an explanation.

To follow hydration changes in the protein–DNA complex in yet another way, we study the effect of nonionic osmolytes. We observe an almost complete isothermal enthalpy–entropy compensation leading to unchanged binding free energies, and we explain this energetic signature of polyols by an enthalpic “chelate” effect. Since the dynamic aspects are indispensable for a profound understanding of protein–DNA association, we also investigate the effect of salt and osmolytes on the rates of association and dissociation of the Tn916–DNA complex.

MATERIALS AND METHODS

Buffers. Experiments were carried out in sodium phosphate/NaCl buffer, pH 6.0, with varying concentrations of Na^+ in the range 0.12–0.32 M; phosphate was kept constant at 0.08 M.

Overexpression and Purification of Int-DBD. The subcloning of Int-DBD comprising residues 2–74 (Cys57Ala), protein expression and purification have been described elsewhere (31, 34). The homogeneity of the protein preparation was checked by mass spectrometry. The protein was dialyzed extensively against the working buffer and its concentration was measured by UV absorption at 280 nm in 6 M GdmCl using ϵ_{280} of $10.81 \text{ mM}^{-1} \text{ cm}^{-1}$ (35).

Preparation of DNA Duplex. Single-stranded oligonucleotides were purchased from Metabion GmbH (Martinsried). For duplex preparation, equimolar amounts of the complementary strands 5'-GAGTAGTAAATTC-3' and 5'-GAATT-TACTACTC-3' were mixed and annealed by heating to 70 °C and slow cooling to room temperature. Concentrations were determined after digestion by phosphodiesterase I (Sigma) from light absorption at 260 nm.

Circular Dichroism Measurements. Measurements were carried out on a Jasco J-715 instrument equipped with a computer-controlled water bath using jacketed cylindrical cells of 1 or 10 mm path length. Thermal unfolding curves were measured by following the ellipticity change during continuous heating from 3 to 65–85 °C at a scan rate of 0.5 or 1 °C min^{-1} with data collection every 20 s. Reversibility of unfolding was checked by repeated scans and was always better than 95%. Thermal melting curves were analyzed as described (34).

Isothermal Titration Calorimetry. Experiments were performed on the VP-ITC instrument (MicroCal Inc., Northampton, MA). The calorimeter was calibrated according to the manufacturer's instruction. Samples of protein and DNA were prepared in and thoroughly dialyzed against the same batch of buffer to minimize artifacts due to minor differences in buffer composition. Concentration was determined after dialysis. The sample cell (1.4 mL) was loaded with 15–70 μM DNA duplex. A titration experiment typically consisted of 20–25 injections of a 150–700 μM protein stock solution, each of 8 or 12 μL volume and 10 or 12 s duration, with a 5 min interval between additions. Stirring rate was 300 rpm. Nonspecific heat effects were estimated from the magnitude of the peaks appearing after complete saturation. Raw data were integrated, corrected for nonspecific heats, normalized for concentration, and analyzed according to a 1:1 binding model assuming a single set of identical binding sites (36).

Fluorescence Stopped-Flow Experiments. The rate of protein–DNA association was measured at 7 °C with the SX.18MV-R stopped-flow spectrometer (Applied Photophysics, Surrey, U.K.). Equal volumes of equally concentrated protein and DNA solutions were mixed (dead time < 3 ms), and the time course of the fluorescence emission above 320 nm was followed upon excitation at 280 nm. Five or more firings were averaged for each kinetic trace. Data were analyzed by nonlinear regression analysis according to a fitting model for simultaneous determination of the rates of binding (k_{on}) and dissociation (k_{off}) from an association experiment as follows (37): Protein (P) and DNA (D) form the complex PD according to



where k_{on} and k_{off} are the rate constants of association and dissociation, respectively. If P and D are mixed in 1:1 molar

and volume ratio, the disappearance of unbound P (or unbound D) can be described by

$$-\frac{d[P]}{dt} = -\frac{d[D]}{dt} = k_{\text{on}}[P][D] - k_{\text{off}}[PD] = k_{\text{on}}[P]^2 - k_{\text{off}}[PD] \quad (2)$$

At time zero $[P] = [D] = [P_0]$. After substitution of $[PD]$ by $[P_0] - [P]$ and rearranging, the decrease of $[P]$ is given by

$$-\frac{d[P]}{dt} = k_{\text{on}}[P_0] \left(\frac{[P]^2}{[P_0]} + \frac{k_{\text{off}}[P]}{k_{\text{on}}[P_0]} - \frac{k_{\text{off}}}{k_{\text{on}}} \right) \quad (3)$$

and after integration,

$$[P] = \left(\frac{zb + zs - b + s}{1 - z} \right) \frac{[P_0]}{2} \quad (4)$$

where

$$b = \frac{k_{\text{off}}}{k_{\text{on}}[P_0]} \quad (5a)$$

$$s = \sqrt{4b + b^2} \quad (5b)$$

$$z = \left(\frac{2 + b - s}{2 + b + s} \right) \exp(-k_{\text{on}}[P_0]) \quad (5c)$$

The time course of the fluorescence change is described by

$$F(t) = F_0 + \Delta F_{\text{max}} \left(1 - \frac{[P]}{[P_0]} \right) \quad (6)$$

where F_0 and ΔF_{max} are the fluorescence at time zero and the maximum change of fluorescence, respectively. The reported kinetic constants represent means from three to four experiments with final concentrations of the complex in the range 0.5–5 μM (50–85% protein–DNA complex at equilibrium).

RESULTS

Salt Dependence of the Stability of Int-DBD and the DNA Duplex. To check for salt-dependent changes of the stability of the free protein and the free DNA, CD melting experiments were performed in the presence of 0.32 M Na^+ , the highest salt concentration used in the ITC experiments. The protein melts at 47 °C, 3 °C higher than in 0.12 M Na^+ (34). The unfolding enthalpies in 0.32 and 0.12 M Na^+ are identical within error. Assuming the same unfolding heat capacity change at both salt concentrations, Int-DBD is marginally stabilized by 0.32 M Na^+ . The melting temperature of the DNA duplex is higher by 5.5 °C in 0.32 M $[\text{Na}^+]$. DNA stabilization is entropic, as expected (1).

Thermodynamics of Complex Formation at Different Salt Concentrations. Isothermal calorimetric titrations of the DNA duplex with Int-DBD were performed at 25 °C. The upper limit of Na^+ concentration was at 0.32 M since the protein tends to aggregate at higher salt concentrations. The stoichiometry was one Int-DBD bound per one 13 bp duplex. Representative experiments are shown in Figure 1, and the thermodynamic parameters of binding are summarized in

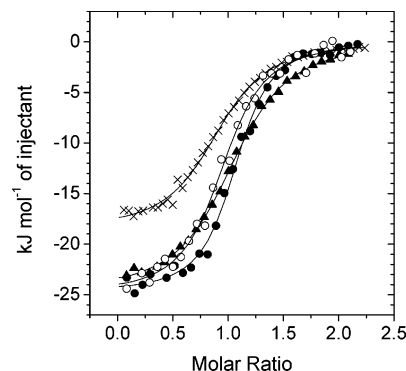
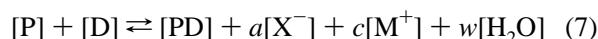


FIGURE 1: Binding isotherms measured by ITC for the titration of Int-DBD to the 13 bp DNA duplex. Titrations were performed at 25 °C in 0.08 M phosphate buffer, pH 6.0, supplemented with 0.12 (●), 0.14 (○), 0.19 (▲) and 0.32 M (×) NaCl. Solid lines are best nonlinear fits to a 1:1 binding model.

Table 1. Binding strongly depends on salt, the association constant determined by ITC, $K_{\text{A}}^{\text{ITC}}$, decreasing 20 times from 0.12 to 0.32 M Na^+ (Table 1). The salt effect may be formalized as (3):



where $[P]$, $[D]$ and $[PD]$ are the molar equilibrium concentrations of protein, DNA, and complex, respectively, $[X^-]$, $[M^+]$, and $[\text{H}_2\text{O}]$ are the molar concentrations of bound anions, cations, and water, respectively, and a , c , and w are stoichiometric coefficients. The following relationship has been proposed for SK_{obs} , which is the change of the observed equilibrium association constant, K_{obs} , with the salt concentration $[\text{MX}]$ (3):

$$\text{SK}_{\text{obs}} = \left(\frac{\partial \ln K_{\text{obs}}}{\partial \ln [\text{MX}]} \right)_{T,p} = - \left[a + c - w \frac{2[\text{MX}]}{[\text{H}_2\text{O}]} \right] \quad (8)$$

The effect of anions (a) expelled from the protein surface is believed to be negligible at low salt concentrations (3). The last term of eq 8 accounts for increased osmotic pressure at high salt concentration. At low salt concentration, the osmotic effect is negligible, and in the absence of an anion effect, the number of cations (Z) released from the DNA is obtained from the simplified form of eq 8:

$$\text{SK}_{\text{obs}} = \left(\frac{\partial \ln K_{\text{obs}}}{\partial \ln [\text{MX}]} \right)_{T,p} = -Z\psi \quad (9)$$

Figure 2 shows the values of $K_{\text{A}}^{\text{ITC}}$ (Table 1) plotted according to eq 9. Using $\Psi = 0.64$, a value deemed appropriate for a short DNA duplex (38, 39), the number of Na^+ ions released from the DNA upon complex formation is $Z = 4.8 \pm 0.2$.

The free energy, enthalpy, and entropy are also linear functions of Na^+ concentration with slopes of $\partial \Delta G / \partial \log [\text{Na}^+] = 17.5 \pm 0.4$, $\partial \Delta H / \partial \log [\text{Na}^+] = 11.9 \pm 0.8$ and $\partial T\Delta S / \partial \log [\text{Na}^+] = -5.6 \pm 0.9$ (Figure 3). Obviously, the enthalpic contribution to the salt effect dominates the observed change of the free binding energy. The enthalpy change at 0.32 M Na^+ was measured at 4.5 and 25 °C. The heat capacity change, calculated from $\partial \Delta H / \partial T$, is $\Delta C_p = 1.8 \pm 0.2 \text{ kJ K}^{-1} \text{ mol}^{-1}$, the same as ΔC_p measured at 0.12 M Na^+ (33).

Table 1: Thermodynamic and Kinetic Parameters for the Association of Int-DBD with a 13 bp Duplex DNA at Different Salt and Polyol Concentrations Observed by ITC and Fluorescence Stopped-Flow Kinetic Measurements^a

conc of additive (M)	ΔH (kJ mol ⁻¹)	$T\Delta S$ (kJ mol ⁻¹)	ΔG (kJ mol ⁻¹)	$K_A^{\text{ITC}} \times 10^{-6}$ (M ⁻¹)	$k_{\text{on}} \times 10^{-8}$ (M ⁻¹ s ⁻¹)	k_{off} (s ⁻¹)	$K_A^{\text{kin}} \times 10^{-7}$ (M ⁻¹)
Na ⁺							
0.12	-25.3 ± 0.9	12.2 ± 0.5	-37.5 ± 0.3	3.72 ± 0.35	5.27 ± 1.58	19.2 ± 9.6	2.74 ± 1.60
0.14	-24.4 ± 0.8	12.4 ± 0.9	-36.8 ± 0.4	2.91 ± 0.48	2.95 ± 1.20	16.8 ± 6.7	1.75 ± 0.90
0.15	-24.1 ± 1.0	12.2 ± 0.6	-36.3 ± 0.3	2.35 ± 0.30	1.52 ± 0.50	11.2 ± 3.4	1.36 ± 0.61
0.19	-22.8 ± 0.9	11.6 ± 1.1	-34.4 ± 0.7	1.06 ± 0.30	0.95 ± 0.28	12.0 ± 5.4	0.79 ± 0.42
0.24	-21.9 ± 0.4	10.4 ± 0.5	-32.3 ± 0.2	0.45 ± 0.04	0.44 ± 0.17	19.7 ± 5.9	0.22 ± 0.11
0.32	-20.2 ± 0.7	10.2 ± 0.8	-30.4 ± 0.4	0.21 ± 0.03	0.23 ± 0.15	26.9 ± 13.4	0.1 ± 0.08
Glycerol							
1.74	-30.5 ± 1.0	6.8 ± 1.3	-37.4 ± 0.9	3.57 ± 0.4	1.04 ± 0.41	6.20 ± 2.80	1.64 ± 0.98
3.34	-37.5 ± 0.9	0.4 ± 0.9	-37.9 ± 0.2	4.37 ± 0.3	0.49 ± 0.19	4.20 ± 1.70	1.17 ± 0.65
Sorbitol							
0.78	-30.8 ±	6.2 ± 1.3	-37.0 ± 0.4	3.06 ± 0.4	<i>b</i>	<i>b</i>	<i>b</i>
1.57	-36.9 ± 0.5	0.2 ± 0.6	-37.1 ± 0.3	3.13 ± 0.3	0.40 ± 0.10	2.36 ± 0.50	1.70 ± 0.68
2.05	-45.8 ± 1.1	-7.3 ± 1.2	-38.5 ± 0.4	5.63 ± 0.4	<i>b</i>	<i>b</i>	<i>b</i>
2.53	-51.0 ± 0.9	-12.5 ± 0.9	-38.5 ± 0.3	5.55 ± 0.5	0.21 ± 0.08	1.14 ± 0.30	1.83 ± 0.80

^a ITC experiments were conducted at 25 °C, pH 6. Kinetic data were collected at 7 °C. NaCl concentration in the presence of glycerol was 0.15 M. The uncertainty of ΔH , K_A^{ITC} , k_{on} , and k_{off} is given as the standard error. The errors of other parameters were calculated as follows:

$$\delta\Delta G = RT(\delta K_A^{\text{ITC}}/K_A^{\text{ITC}}); \quad \delta T\Delta S = \sqrt{(\delta\Delta H)^2 + (\delta\Delta G)^2}; \quad \delta K_A^{\text{kin}} = K_A^{\text{kin}} \sqrt{\left(\frac{\delta k_{\text{on}}}{k_{\text{on}}}\right)^2 + \left(\frac{\delta k_{\text{off}}}{k_{\text{off}}}\right)^2}. \quad ^b \text{ Not determined.}$$

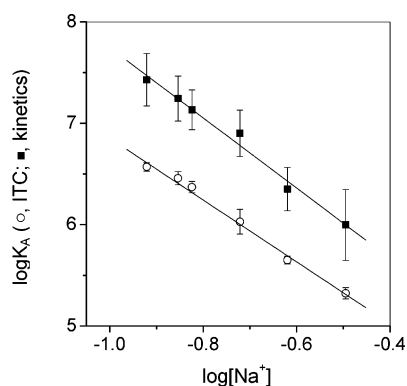


FIGURE 2: Salt dependence of the equilibrium constant for the binding of Int-DBD to the 13 bp DNA duplex. Open circles are data obtained by ITC at 25 °C. Solid squares are $\log(K_A^{\text{kin}}) = \log(k_{\text{on}}/k_{\text{off}})$ obtained from fluorescence stopped-flow experiments at 7 °C. Continuous lines are linear best fits according to eq 9. The slopes, SK_{obs} (eq 9), are -3.07 ± 0.2 for the ITC data and -3.46 ± 0.5 for the kinetic data.

Titration experiments were also conducted in the presence of Br⁻ (open symbols in Figure 3). Binding is slightly weaker in the presence of Br⁻. However, the salt dependence of K_A for NaCl and NaBr is the same. Although, the enthalpy–entropy partitioning of ΔG is different, the slopes of plots of ΔH versus $\log [\text{Na}^+]$ and $T\Delta S$ versus $\log [\text{Na}^+]$ are quite close. (Figure 3).

Thermodynamics of Complex Formation in the Presence of Osmolytes. The effect of glycerol and sorbitol at $[\text{Na}^+] = 0.15$ M was measured by ITC at 25 °C. Thermodynamic parameters are presented in Table 1 and Figure 4. The stability of the Int-DBD–DNA complex changes only slightly up to 2.5 M sorbitol and up to 3.3 M glycerol. However, nearly identical ΔG of binding in the absence and presence of osmolytes is hiding large compensatory decreases of binding enthalpy and entropy. Association is enthalpically more favorable in the presence of polyol, but this enthalpy decrease is almost perfectly compensated by an unfavorable decrease of the binding entropy.

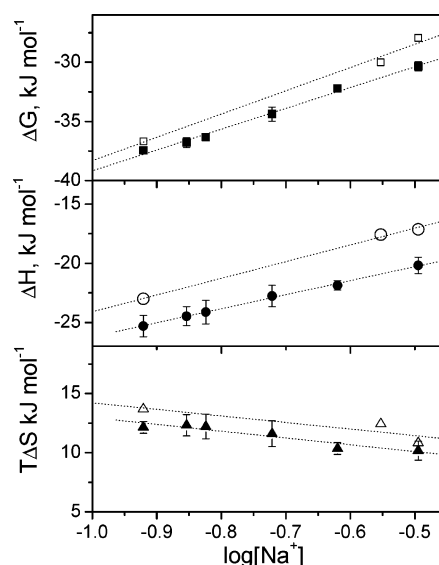


FIGURE 3: Dependence of thermodynamic quantities ΔG (top), ΔH (middle), and $T\Delta S$ (bottom) on $\log [\text{NaCl}]$ (filled symbols) and $\log [\text{NaBr}]$ (open symbols). Data were obtained by ITC at 25 °C and pH 6.0. Dotted lines are linear fits.

Kinetics of Int-DBD–DNA Binding. Stopped-flow measurements were performed in the same range of salt concentrations as those used in the ITC experiments. The observed half-times of complex formation vary with protein and DNA concentration, and the kinetic traces are well described by the simple bimolecular reaction of eq 1. Since the half-times of association and dissociation were similar under the chosen reaction conditions and since less than 100% of complex was formed at equilibrium, the association and dissociation rate constants could be obtained from single reaction traces (11, 37). Representative kinetic traces are shown in Figure 5. The rate of bimolecular association, k_{on} , is substantially reduced by increasing the salt concentration; the decrease is exponential from $(5.2 \pm 1.6) \times 10^8 \text{ M}^{-1} \text{ s}^{-1}$ at 0.12 M Na⁺ to $(2.3 \pm 1.5) \times 10^7 \text{ M}^{-1} \text{ s}^{-1}$ at 0.32 M Na⁺. The rate of dissociation, k_{off} , scatters around $15 \pm 10 \text{ s}^{-1}$.

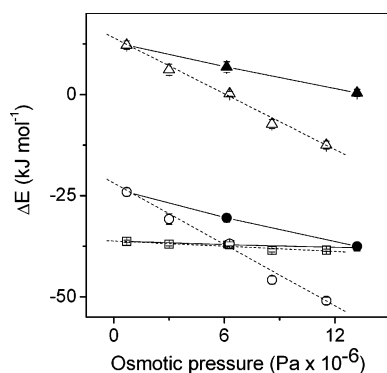


FIGURE 4: Effect of glycerol and sorbitol on ΔG (\square), ΔH (\circ), and $T\Delta S$ (Δ). Data were obtained by ITC at 25 °C and pH 6.0 in the presence of 0.15 M NaCl. Filled symbols and continuous lines represent data obtained in the presence of glycerol. Open symbols and dashed lines represent data obtained in the presence of sorbitol.

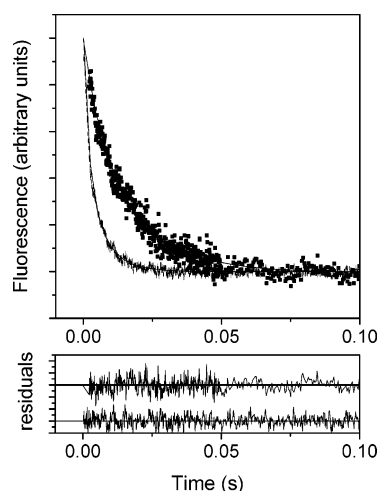


FIGURE 5: Representative kinetic traces describing the formation of the Int-DBD–DNA complex. Experiments were performed at 7 °C in phosphate buffer, pH 6.0. Final protein and duplex concentrations were 1 μ M. The concentration of Na^+ was 0.32 (top trace) and 0.12 M (bottom trace). The lower panels show the residuals from nonlinear least-squares fits according to the combined eqs 4–6.

Plots of $\log(k_{\text{on}})$ and $\log(k_{\text{off}})$ against $\log [\text{Na}^+]$ are linear, having slopes of -3.01 ± 0.32 and 0.47 ± 0.38 , respectively (Figure 6). The equilibrium constants calculated from the kinetic data as $K_{\text{A}}^{\text{kin}} = k_{\text{on}}/k_{\text{off}}$ exhibit the same salt dependence as $K_{\text{A}}^{\text{ITC}}$ (parallel slopes in Figure 2). The number of cations displaced from the binding interface is $Z = 5.4 \pm 0.5$ from the salt dependence of $K_{\text{A}}^{\text{kin}}$, which compares well with $Z = 4.8 \pm 0.2$ from the salt dependence of $K_{\text{A}}^{\text{ITC}}$. The kinetic analysis reveals that high salt destabilizes the protein–DNA complex by slowing the rate of association, the dissociation rate remaining unchanged. We note that $K_{\text{A}}^{\text{kin}}$ is consistently higher than $K_{\text{A}}^{\text{ITC}}$ (Figure 2). The reason for this discrepancy between kinetic and thermodynamic equilibrium values is not clear and cannot be attributed to a temperature dependence of the binding constant (33). Disparity between K_{A} obtained by calorimetry and fluorescence spectroscopy has been observed before (40, 41).

The rates of association and dissociation were determined in buffers containing glycerol and sorbitol. Both k_{on} and k_{off} decrease in parallel with increasing osmolyte concentration (Figure 5 and Table 1). As a consequence, $K_{\text{A}}^{\text{kin}}$ is very

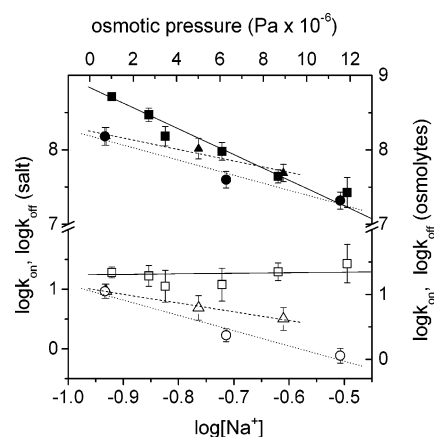


FIGURE 6: Effect of salt and glycerol on the rates of association and dissociation. Rate constants of association (k_{on} , filled symbols) and dissociation (k_{off} , open symbols) were determined by fluorescence stopped-flow at 7 °C. Straight lines represent linear best fits. Squares and continuous lines (bottom x-axis, left y-axis) represent data obtained in the presence of different Na^+ concentrations. Triangles and dashed lines (top x-axis, right y-axis) represent data obtained in the presence of glycerol and 0.15 M Na^+ . Circles and dotted lines represent data obtained in the presence of sorbitol and 0.15 M Na^+ .

similar in the presence and absence of osmolytes, confirming the very small effect of these substances on G seen in ITC.

DISCUSSION

Energetic Partitioning of the Salt Effect. Experimental results on the effect of salt on protein–DNA binding are commonly treated in terms of the classic counteraction/limiting law model (CC/LL; (1–3)). Binding releases counterions that are condensed around the macromolecules as described by eq 8. In a series of classical experiments, Record and colleagues investigated the binding of short cationic peptides to DNA (9) and formulated eqs 8 and 9, which hold for many protein–DNA systems (3). Application of eq 9 predicts that 5.1 ± 0.5 cations are expelled from the interface of the Int-DBD–DNA complex (mean Z-value from ITC and kinetics). This number is in good agreement with structural data. There are seven arginine and lysine side chains contacting DNA in the complex, five are bonded to phosphate groups and two to nucleotide bases (31, 32). The DNA phosphates bind Na^+ ions, which in the complex are (partly) displaced by positively charged side chains of the protein.

According to the CC/LL model, weaker binding at higher salt concentration originates from the less favorable cratic entropy of expelling DNA-associated cations into the bulk solution, that is, from changing $c[\text{M}^+]$ in eq 7 (1, 2). At high salt concentration, there is less entropy gain from cation displacement. The enthalpic term of the salt-dependent free energy change is believed to be close to zero, as inferred from the binding of polylysines and polyamines to DNA being independent of temperature at different salt concentrations (9). In contrast, we find that the loss of enthalpy dominates the salt effect, the loss of entropy being smaller.

What causes the strong enthalpic destabilization by salt of the Int-DBD–DNA complex? One possibility is release of specifically bound anions from Int-DBD causing an increase of enthalpy. In this case the enthalpy change should be ion-specific, yet in our experiments ΔH depends in the

same way on Cl^- and Br^- . The release of specifically bound ions should also be temperature-dependent yet ΔC_p of complex formation is independent of the salt concentration. Thus, we can rule out a *specific* anion effect as a major cause of the large enthalpy increase induced by salt.

The enthalpic weakening of the Int-DBD–DNA complex by salt can be explained in the framework of more recent views on the nature of the general salt effect.² Direct evaluation of the electrostatic solvation free energy of polyelectrolytes applying the nonlinear Poisson–Boltzmann (PB) equation predicts that the general salt effect, that is, the release of nonspecifically bound ions, weakens binding in terms of both enthalpy and entropy (4, 42–44). In the PB model, the counterion atmosphere is regarded as a single, continuous layer the density of which decreases gradually in the direction perpendicular to the DNA duplex axis. The principal sources of enthalpic destabilization are the salt-dependent electrostatic (Coulombic) enthalpy change and the change of the dielectric constant caused by enhanced water mobility due to the disruption of the ion cloud around the DNA.

Exclusion of counterions more distant from the DNA will be entropically less favorable because their mobility is less restricted, while the enthalpic effect of removing the same counterions is still sizable because the strong electrostatic field of DNA is long-range. In other words, when moving away from the DNA, the entropy gain falls more rapidly than the Coulombic enthalpy loss. Furthermore, ions tightly associated with the duplex are significantly dehydrated. Expulsion of such ions might be linked to a small enthalpic effect since the favorable enthalpy of ion hydration counteracts the Coulombic enthalpy loss. More distant ions are better hydrated and the Coulombic enthalpy dominates the net effect. Therefore, the enthalpy–entropy partitioning of the general salt effect depends on the volume excluded by the protein in the protein–DNA complex. In other words, the interaction area and volume of the protein domain bound to the DNA determine the degree of enthalpy–entropy partitioning. Lack of a salt-dependent enthalpy increase in the classical experiments of Record and co-workers (2, 9) could be due to the much smaller excluded volume and higher flexibility of pentyllysine compared to typical DNA-binding domains of proteins. Further experimental and theoretical work is needed to support this interpretation.

Binding Energetics in the Presence of Nonionic Polyol Osmolytes. Osmolytes can be used to estimate the number of water molecules participating in macromolecular association (27–29). For a protein–DNA complex, only nonionic

osmolytes should be used since ionic osmolytes would also yield a salt effect. In view of our previous evidence for water at the contact site between Int-DBD and DNA (33, 45), a significant osmotic effect of glycerol and sorbitol on the stability of the complex was expected but not confirmed by the present experiments. One possible reason is that the osmolyte concentrations used may not have caused sufficient osmotic stress to release water from the binding site. The Int-DBD–DNA complex is rather flexible, and water is exchanged rapidly (45). No water molecules in stable cavities or deep crevices permanently disconnected from the bulk solvent are seen in our MD simulations (45). Instead, most of the water molecules bridging the protein and the DNA form clusters that are chained to the bulk water. Higher osmotic stress might have been necessary to release such rapidly exchanging water. (Higher osmolyte concentrations lead to experimental artifacts.)

Nonetheless, there are significant but compensatory changes of the enthalpy and entropy of association induced by osmolytes (Figure 4). Two explanations for this intriguing polyol-induced enthalpy–entropy compensation can be put forward. First, transferring nonpolar groups from water into solutions containing glycerol or sorbitol produces positive changes of enthalpy and entropy, while the transfer of polar groups leads to negative changes (46). Therefore, burial of nonpolar surface at the protein–DNA interface in the presence of osmolyte favors binding enthalpically (binding is more exothermic) and disfavors binding entropically. Burial of polar surface acts in the opposite way. Since more nonpolar surface is shielded in the Int-DBD–DNA complex, the transfer of more nonpolar than polar groups from the osmolyte solution to the protein–DNA contact site leads to a compensatory decrease of enthalpy and entropy. However, this explanation accounts for only a fraction of the entire enthalpy–entropy effect of the osmolyte.³ We propose an *enthalpic chelate effect* as a second contributor to the remarkable enthalpy–entropy compensation. In a general context, a chelate effect reflects the phenomenon of positive cooperativity: the summed energy of individual noncovalent bonds is less than the energy driving a multipoint binding process (47–49). The classical chelate effect is entropic since the first bond formed between two molecules eliminates the entropic penalty for the formation of subsequent bonds. However, multipoint binding also causes damping of intermolecular motions. Less molecular motion facilitates the formation of noncovalent bonds and produces a favorable enthalpic component to binding; this is called an enthalpic chelate effect (48). Now, it is well-known that polyols restrict local and global conformational flexibility and thermal motions of proteins (50–53). Glycerol decreases the specific volume and the adiabatic compressibility of native proteins, possibly by causing the collapse of voids in the protein molecule (54, 55). Glycerol and sorbitol strengthen hydrophobic interactions in general (56). Restricting the flexibility of the protein–DNA complex by the osmolyte may intensify packing interactions and may thereby increase the enthalpy of binding by an enthalpic chelate effect. On the other hand,

² The general salt effect describes the contribution of salt to the free energy of charging the DNA: $\Delta G_S = \Delta G_{\text{im}} + \Delta G_{\text{ii}} + \Delta G_{\text{org}}$. The salt-dependent term (ΔG_S) is decomposed into contributions from ion–macromolecule interactions (ΔG_{im}), ion–ion interactions (ΔG_{ii}), and the cratic entropy associated with ion organization (ΔG_{org}). Both ΔG_{im} and ΔG_{ii} comprise electrostatic (Coulombic) enthalpy and dielectric entropy terms, the latter accounting for the change of the dielectric constant caused by the enhanced water mobility when the ion cloud around the DNA is disrupted. Since the dielectric constant depends on salt and temperature, there will be an enthalpic contribution to ΔG_{im} and ΔG_{ii} . As to ΔG_{org} , which is small and either favorable or unfavorable, it is the sum of the cratic entropy of reorganization of the ion atmosphere and a dielectric entropy term. In the total energetic balance of ΔG_S , the favorable dielectric entropy contribution is larger than the cratic entropy of ion release.

³ The calculation is based on the mean transfer enthalpy and entropy of alanine, valine, leucine, phenylalanine, and tryptophan (to model nonpolar surface), and diglycine (to model polar surface) normalized per \AA^2 and the proportion of polar to nonpolar surface buried at the Int-DBD–DNA interface. Transfer data from ref 46 were used.

a more rigid and less fluctuating complex is entropically disfavored (57). Taken together, osmolyte-induced tightening of the Int-DBD–DNA complex can account for enthalpic stabilization and entropic destabilization and thus for at least part of the observed enthalpy–entropy compensation. A similar observation was made for noncovalent leucine zipper dimers, which are stabilized by enthalpy and destabilized by entropy in the presence of 30% glycerol at room temperature (58).

Solvent Effects on the Kinetics of Association and Dissociation. The salt effect observed by ITC is mirrored by the kinetic data: the lower stability of the Int-DBD–DNA complex in high salt is due to a slower rate of association at an unchanged rate of dissociation. The salt dependence of association can be rationalized in terms of electrostatic effects. DNA has a strong negative electrostatic potential, and Int-DBD is positively charged at its DNA-binding face. Since electrostatics is long-range, the complementarity of electrostatic fields of protein and DNA speeds up association by diffusion. First, the two molecules are “pulled” together by simple electrostatic attraction. Second, the rotational degrees of freedom are restricted in the initial nonspecific encounter complex, and the molecules collide in an approximately correct orientation, so the optimal steric fit required for tight binding is found more rapidly. This effect has been called electrostatic steering (59). Shielding of charges by salt will slow down the formation of the encounter complex and increase the probability for unproductive encounters.

Electrostatic interactions are less important for dissociation because charge–charge (and other polar) interactions suffer a significant energetic penalty from dehydration of the protein–DNA interface. This penalty severely diminishes, and quite often overbalances, the favorable Coulombic charge–charge attraction energy. Computational studies predict that nonpolar contacts are the major contributor to the stability of protein–DNA complexes, and they are much less affected by salt (60). Therefore, the activation barrier for dissociation is largely dominated by the salt-independent disruption of nonpolar interactions. Altogether, the results confirm that in the absence of specific ion binding effects, salt has a small effect on the rate of dissociation and a large effect on the rate of association of a protein–DNA complex.

As to the effect of glycerol and sorbitol on kinetics, the decrease of the association rate is likely due to increased viscosity (61). Indeed, the effect is stronger for sorbitol since the latter is more viscous than glycerol at the same concentration. The observed decrease of the dissociation rate in glycerol is more difficult to understand. In part, it can also be explained by increased viscosity because protein and DNA will diffuse at a lower rate out of the radius of the encounter complex. However, association should be more affected than dissociation in the relatively low concentration regime of the experiments. We propose a nonnegligible contribution from the chelate effect discussed above. Tightening of the complex by the osmolyte might increase the activation barrier for dissociation of a macromolecular complex stabilized by multipoint weak interactions.

CONCLUSIONS

After our previous investigation demonstrating conformational adaptation and partial dehydration in the Int-DBD–

DNA complex (33), we now have studied the effect of salt and polyol osmolytes on this protein–DNA complex characterized by a three-stranded β -sheet fitting into the major groove of the DNA. As expected, salt lowers the stability of the complex. We find that destabilization is caused primarily by a loss of binding enthalpy and not by a large loss of binding entropy. We argue that enthalpy–entropy partitioning is influenced by the size of the protein and the surface area that it occludes on the DNA. The larger the solvent volume excluded by the DNA-bound protein, the more important is the salt-induced enthalpy loss and the less important the loss of entropy. Weakening of the Int-DBD–DNA complex by salt is confirmed by kinetic data: salt decreases the rate of association and leaves the rate of dissociation unchanged, an observation in agreement with complex formation by electrostatic steering.

The observed osmolyte effect is more difficult to explain. Glycerol and sorbitol have a small effect on the stability of the Int-DBD–DNA complex, but there is a large polyol-induced enthalpy–entropy compensation: the binding enthalpy increases, and the binding entropy decreases. The remarkable enthalpy–entropy effect of the polyols may be caused in part by an enthalpic chelate effect. By this we mean that osmolytes tighten the structure of the Int-DBD–DNA complex whereby the formation of enthalpically favorable noncovalent interactions is promoted at the entropic cost of a more rigid complex. The osmolyte effect is again supported by kinetic data showing parallel decreases of association and dissociation rates. This work helps to clarify the intricate thermodynamic mechanisms underlying the specific formation of protein–DNA complexes.

ACKNOWLEDGMENT

We thank Dr. Alemayehu Gorfe for helpful discussions.

REFERENCES

1. Manning, G. S. (1978) The molecular theory of polyelectrolyte solutions with applications to the electrostatic properties of polynucleotides, *Q. Rev. Biophys.* 11, 179–246.
2. Record, M. T., Jr., Lohman, M. L., and De Haseth, P. (1976) Ion effects on ligand–nucleic acid interactions, *J. Mol. Biol.* 107, 145–158.
3. Record, M. T., Jr., Ha, J. H., and Fisher, M. A. (1991) Analysis of equilibrium and kinetic measurements to determine thermodynamic origins of stability and specificity and mechanism of formation of site-specific complexes between proteins and helical DNA, *Methods Enzymol.* 208, 291–343.
4. Sharp, K. A., Friedman, R. A., Misra, V., Hecht, J., and Honig, B. (1995) Salt effects on polyelectrolyte–ligand binding: comparison of Poisson–Boltzmann, and limiting law/counterion binding models, *Biopolymers* 36, 245–262.
5. Bergqvist, S., O’Brien, R., and Ladbury, J. E. (2001) Site-specific cation binding mediates TATA binding protein–DNA interaction from a hyperthermophilic archaeon, *Biochemistry* 40, 2419–2425.
6. Bergqvist, S., Williams, M. A., O’Brien, R., and Ladbury, J. E. (2004) Heat capacity effects of water molecules and ions at a protein–DNA interface, *J. Mol. Biol.* 336, 829–842.
7. Frank, D. E., Saecker, R. M., Bond, J. P., Capp, M. W., Tsodikov, O. V., Melcher, S. E., Levandoski, M. M., and Record, M. T., Jr. (1997) Thermodynamics of the interactions of lac repressor with variants of the symmetric lac operator: effects of converting a consensus site to a nonspecific site, *J. Mol. Biol.* 267, 1186–1206.
8. Hart, D. J., Speight, R. E., Cooper, M. A., Sutherland, J. D., and Blackburn, J. M. (1999) The salt dependence of DNA recognition by NF- κ B p50: a detailed kinetic analysis of the effects on affinity and specificity, *Nucleic Acids Res.* 27, 1063–1069.

9. Lohman, T. M., Dehaseth, P. L., and Record, M. T. (1980) Pentalysine-Deoxyribonucleic Acid Interactions — a Model for the General Effects of Ion Concentrations on the Interactions of Proteins with Nucleic Acids, *Biochemistry* 19, 3522–3530.
10. Kozlov, A. G., and Lohman, T. M. (2000) Large contributions of coupled protonation equilibria to the observed enthalpy and heat capacity changes for ssDNA binding to *Escherichia coli* SSB protein, *Proteins* (Suppl. 4), 8–22.
11. Kozlov, A. G., and Lohman, T. M. (2002) Stopped-flow studies of the kinetics of single-stranded DNA binding and wrapping around the *Escherichia coli* SSB tetramer, *Biochemistry* 41, 6032–6044.
12. Lohman, T. M., Overman, L. B., Ferrari, M. E., and Kozlov, A. G. (1996) A highly salt-dependent enthalpy change for *Escherichia coli* SSB protein-nucleic acid binding due to ion-protein interactions, *Biochemistry* 35, 5272–5279.
13. Lundback, T., and Hrd, T. (1996) Salt dependence of the free energy, enthalpy, and entropy of nonsequence specific DNA binding, *J. Phys. Chem.* 100, 17690–17695.
14. O'Brien, R., DeDecker, B., Fleming, K. G., Sigler, P. B., and Ladbury, J. E. (1998) The effects of salt on the TATA binding protein-DNA interaction from a hyperthermophilic archaeon, *J. Mol. Biol.* 279, 117–125.
15. Oda, M., Furukawa, K., Ogata, K., Sarai, A., and Nakamura, H. (1998) Thermodynamics of specific and nonspecific DNA binding by the c-Myb DNA-binding domain, *J. Mol. Biol.* 276, 571–590.
16. Oda, M., Furukawa, K., Sarai, A., and Nakamura, H. (1999) Kinetic analysis of DNA binding by the c-Myb DNA-binding domain using surface plasmon resonance, *FEBS Lett.* 454, 288–292.
17. Poon, G. M. K., and MacGregor, R. B. (2004) A thermodynamic basis of DNA sequence selectivity by the ETS domain of murine PU.1, *J. Mol. Biol.* 335, 113–127.
18. Seimiya, M., and Kurosawa, Y. (1996) Kinetics of binding of Antp homeodomain to DNA analyzed by measurements of surface plasmon resonance, *FEBS Lett.* 398, 279–284.
19. Schwabe, J. W. (1997) The role of water in protein-DNA interactions, *Curr. Opin. Struct. Biol.* 7, 126–134.
20. Billeter, M., Guntert, P., Luginbuhl, P., and Wuthrich, K. (1996) Hydration and DNA recognition by homeodomains, *Cell* 85, 1057–1065.
21. Chillemi, G., Castrignano, T., and Desideri, A. (2001) Structure and hydration of the DNA-human topoisomerase I covalent complex, *Biophys. J.* 81, 490–500.
22. Duan, J., and Nilsson, L. (2002) The role of residue 50 and hydration water molecules in homeodomain DNA recognition, *Eur. Biophys. J.* 31, 306–316.
23. Reddy, C. K., Das, A., and Jayaram, B. (2001) Do water molecules mediate protein-DNA recognition? *J. Mol. Biol.* 314, 619–632.
24. Shakked, Z., Guzikevichgurestein, G., Frolov, F., Rabinovich, D., Joachimiak, A., and Sigler, P. B. (1994) Determinants of Repressor-Operator Recognition from the Structure of the Trp Operator Binding-Site, *Nature* 368, 469–473.
25. Joachimiak, A., Haran, T. E., and Sigler, P. B. (1994) Mutagenesis Supports Water Mediated Recognition in the Trp Repressor-Operator System, *EMBO J.* 13, 367–372.
26. Parsegian, V. A., Rand, R. P., and Rau, D. C. (1995) Macromolecules and water: Probing with osmotic stress, *Methods Enzymol.* 259, 43–94.
27. Parsegian, V. A., Rand, R. P., and Rau, D. C. (2000) Osmotic stress, crowding, preferential hydration, and binding: A comparison of perspectives, *Proc. Natl. Acad. Sci. U.S.A.* 97, 3987–3992.
28. Timasheff, S. N., and Arakawa, T. (1988) Mechanism of Protein Precipitation and Stabilization by Co-Solvents, *J. Cryst. Growth* 90, 39–46.
29. Timasheff, S. N. (2002) Protein-solvent preferential interactions, protein hydration, and the modulation of biochemical reactions by solvent components, *Proc. Natl. Acad. Sci. U.S.A.* 99, 9721–9726.
30. Scott, J. R., and Churchward, G. G. (1995). Conjugative Transposition. *Annu. Rev. Microbiol.* 49, 367–397.
31. Wojciak, J. M., Connolly, K. M., and Clubb, R. T. (1999) NMR structure of the Tn916 integrase-DNA complex, *Nat. Struct. Biol.* 6, 366–373.
32. Connolly, K. M., Ilangovan, U., Wojciak, J. M., Iwahara, M., and Clubb, R. T. (2000) Major groove recognition by three-stranded beta-sheets: Affinity determinants and conserved structural features, *J. Mol. Biol.* 300, 841–856.
33. Milev, S., Gorfe, A. A., Karshikoff, A., Clubb, R. T., Bosshard, H. R., and Jelesarov, I. (2003) Energetics of sequence-specific Protein-DNA association: Binding of integrase Tn916 to its target DNA, *Biochemistry* 42, 3481–3491.
34. Milev, S., Gorfe, A. A., Karshikoff, A., Clubb, R. T., Bosshard, H. R., and Jelesarov, I. (2003) Energetics of sequence-specific protein-DNA association: Conformational stability of the DNA binding domain of integrase Tn916 and its cognate DNA duplex, *Biochemistry* 42, 3492–3502.
35. Edelhoch, H. (1967) Spectroscopic Determination of Tryptophan and Tyrosine in Proteins, *Biochemistry* 6, 1948–1954.
36. Wiseman, T., Williston, S., Brandts, J. F., and Lin, L. N. (1989) Rapid Measurement of Binding Constants and Heats of Binding Using a New Titration Calorimeter, *Anal. Biochem.* 179, 131–137.
37. Wendt, H., Leder, L., Harma, H., Jelesarov, I., Baici, A., and Bosshard, H. R. (1997) Very rapid, ionic strength-dependent association and folding of a heterodimeric leucine zipper, *Biochemistry* 36, 204–213.
38. Dragan, A. I., Liggins, J. R., Crane-Robinson, C., and Privalov, P. L. (2003) The energetics of specific binding of AT-hooks from HMGAI to target DNA, *J. Mol. Biol.* 327, 393–411.
39. Olmsted, M. C., Bond, J. P., Anderson, C. F., and Record, M. T. (1995) Grand-Canonical Monte Carlo Molecular and Thermodynamic Predictions of Ion Effects on Binding of an Oligocation (L(8+)) to the Center of DNA Oligomers, *Biophys. J.* 68, 634–647.
40. Jelesarov, I., and Bosshard, H. R. (1994) Thermodynamics of Ferredoxin Binding to Ferredoxin-Nadp(+) Reductase and the Role of Water at the Complex Interface, *Biochemistry* 33, 13321–13328.
41. Lundback, T., and Ladbury, J. E. (1998) Inconsistencies in binding affinities measured using different techniques, *Biophys. J.* 74, A40–A40.
42. Misra, V. K., Hecht, J. L., Sharp, K. A., Friedman, R. A., and Honig, B. (1994) Salt Effects on Protein-DNA Interactions — the Lambda-cl Repressor and EcoRI Endonuclease, *J. Mol. Biol.* 238, 264–280.
43. Sharp, K. A. (1995) Polyelectrolyte electrostatics: Salt dependence, entropic, and enthalpic contributions to free energy in the nonlinear Poisson-Boltzmann model, *Biopolymers* 36, 227–243.
44. Fogolari, F., Elcock, A. H., Esposito, G., Viglino, P., Briggs, J. M., and McCammon, J. A. (1997) Electrostatic effects in homeodomain-DNA interactions, *J. Mol. Biol.* 267, 368–381.
45. Gorfe, A. A., Caflisch, A., and Jelesarov, I. (2004). The role of flexibility and hydration on the sequence-specific DNA recognition by the Tn916 integrase protein: a molecular dynamics analysis, *J. Mol. Recognit.* 17, 120–131.
46. Gekko, K. (1981) Enthalpy and Entropy of Transfer of Amino-Acids and Diglycine from Water to Aqueous Polyol Solutions, *J. Biochem.* 90, 1643–1652.
47. Hunter, C. A., and Tomas, S. (2003) Cooperativity, partially bound states, and enthalpy-entropy compensation, *Chem. Biol.* 10, 1023–1032.
48. Williams, D. H., Stephens, E., and Zhou, M. (2003) Ligand binding energy and catalytic efficiency from improved packing within receptors and enzymes, *J. Mol. Biol.* 329, 389–399.
49. Williams, D. H., Stephens, E., and Zhou, M. (2003) How can enzymes be so efficient? *Chem. Commun.* 1973–1976.
50. Bizzarri, A. R., and Cannistraro, S. (1993) Solvent Modulation of the Structural Heterogeneity in Feiii Myoglobin Samples — a Low-Temperature Epr Investigation, *Eur. Biophys. J. Biophys. Lett.* 22, 259–267.
51. Butler, S. L., and Falke, J. J. (1996) Effects of protein stabilizing agents on thermal backbone motions: A disulfide trapping study, *Biochemistry* 35, 10595–10600.
52. Schlyer, B. D., Steel, D. G., and Gafni, A. (1996) Long time-scale probing of the protein globular core using hydrogen-exchange and room-temperature phosphorescence, *Biochem. Biophys. Res. Commun.* 223, 670–674.
53. Kendrick, B. S., Chang, B. S., Arakawa, T., Peterson, B., Randolph, T. W., Manning, M. C., and Carpenter, J. F. (1997) Preferential exclusion of sucrose from recombinant interleukin-1 receptor antagonist: Role in restricted conformational mobility and compaction of native state, *Proc. Natl. Acad. Sci. U.S.A.* 94, 11917–11922.
54. Priev, A., Almagor, A., Yedgar, S., and Gavish, B. (1996) Glycerol decreases the volume and compressibility of protein interior, *Biochemistry* 35, 2061–2066.

55. Almagor, A., Priev, A., Barshtein, G., Gavish, B., and Yedgar, S. (1998) Reduction of protein volume and compressibility by macromolecular cosolvents: dependence on the cosolvent molecular weight, *Biochim. Biophys. Acta* 1382, 151–156.
56. Kamiyama, T., Sadahide, Y., Nogusa, Y., and Gekko, K. (1999) Polyol-induced molten globule of cytochrome *c*: an evidence for stabilization by hydrophobic interaction, *Biochim. Biophys. Acta* 1434, 44–57.
57. Tidor, B., and Karplus, M. (1994) The Contribution of Vibrational Entropy to Molecular Association – the Dimerization of Insulin, *J. Mol. Biol.* 238, 405–414.
58. Durr, E., and Jelesarov, I. (2000) Thermodynamic analysis of cavity creating mutations in an engineered leucine zipper and energetics of glycerol-induced coiled coil stabilization, *Biochemistry* 39, 4472–4482.
59. von Hippel, P. H., and Berg, O. G. (1989) Facilitated target location in biological systems, *J. Biol. Chem.* 264, 675–678.
60. Jayaram, B., McConnell, K., Dixit, S. B., Das, A., and Beveridge, D. L. (2002) Free-energy component analysis of 40 protein-DNA complexes: A consensus view on the thermodynamics of binding at the molecular level, *J. Comput. Chem.* 23, 1–14.
61. Schreiber, G., and Fersht, A. R. (1996) Rapid, electrostatically assisted association of proteins, *Nat. Struct. Biol.* 3, 427–431.

BI048907N